NANO LETTERS

Letter

pubs.acs.org/NanoLett

Molecular Plasmonics

Adam Lauchner,[†,#] Andrea E. Schlather,[‡,#] Alejandro Manjavacas,[§,#] Yao Cui,[‡,#] Michael J. McClain,[‡,#] Grant J. Stec,[‡,#] F. Javier García de Abajo,[*,∥,⊥] Peter Nordlander,[*,†,§,#] and Naomi J. Halas[*,†,‡,§,#]

[†]Department of Electrical and Computer Engineering, [‡]Department of Chemistry, and [§]Department of Physics and Astronomy, Rice University, Houston, Texas 77005, United States

[∥]ICFO-Institut de Ciencies Fotoniques, Mediterranean Technology Park, 08860 Castelldefels (Barcelona), Spain

[⊥]ICREA-Institució Catalana de Recerca i Estudis Avancats, Passeig Lluís Companys, 23, 08010 Barcelona, Spain

[#]Laboratory for Nanophotonics, Smalley-Curl Institute, Rice University Houston, Texas 77005, United States

S *Supporting Information*

ABSTRACT: Graphene supports surface plasmons that have been observed to be both electrically and geometrically tunable in the mid- to far-infrared spectral regions. In particular, it has been demonstrated that graphene plasmons can be tuned across a wide spectral range spanning from the mid-infrared to the terahertz. The identification of a general class of plasmonic excitations in systems containing only a few dozen atoms permits us to extend this versatility into the visible and ultraviolet. As appealing as this extension might be for active nanoscale manipulation of visible light, its realization constitutes a formidable technical challenge. We experimentally demonstrate the existence of molecular plasmon resonances in the visible for ionized polycyclic aromatic hydrocarbons (PAHs), which we reversibly switch by adding, then removing, a single electron from the molecule. The charged PAHs display intense absorption in the visible regime with electrical and geometrical tunability analogous to the plasmonic resonances of much larger nanographene systems. Finally, we also use the switchable molecular plasmon in anthracene to demonstrate a proof-of-concept low-voltage electrochromic device.

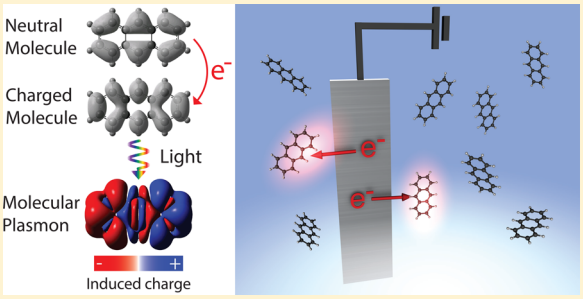

KEYWORDS: *Plasmonics, polycyclic aromatic hydrocarbons, photonics, graphene, electrochemistry, polyacenes*

Collective oscillations of conduction electrons, known as surface plasmons, couple strongly to light and are confined to dimensions substantially below the diffraction limit, giving rise to large near-field enhancements. These properties, together with the strong sensitivity of plasmons to the morphology of the structures, have generated great expectations for technological applications, particularly in optical sensing down to the single-molecule limit.[1−3] Graphene has recently surfaced as an outstanding material for supporting plasmons. In addition to exhibiting strong planar confinement, graphene plasmons have been demonstrated to be electrically tunable in nanoribbons,[4−6] nanodisks,[7] nanorings,[7] and other confined morphologies at mid-infrared and lower frequencies,[6,8−12] scaling as $\sim n^{1/4}/D^{1/2}$ with the doping density n and the lateral size of the structure D. However, many promising applications of plasmonics (e.g., sensing,[2] on-chip communications,[13] and photocatalysis[14]) exploit the visible and near-infrared regions of the spectrum. The extension of graphene plasmons to these higher frequency ranges is thus an important goal, which requires moving toward smaller sizes or higher doping densities.[15,16] Unfortunately, reaching the visible regime with state-of-the-art doping technologies requires patterning graphene down to sizes <10 nm, which is unattainable by currently available top-down fabrication methods. However, this length scale is commensurate with that of polycyclic aromatic molecules, which can readily be obtained in high purity using chemical methods. In particular, polycyclic aromatic hydrocarbons (PAHs) can be regarded as molecular versions of graphene, edge-passivated with hydrogen atoms.[17,18]

Insights from recent time-dependent density functional theory[18−20] (TDDFT) and random phase approximation[21,22] (RPA) theoretical work imply that molecular-scale systems support some excitation modes which are indeed collective in nature. The description of a molecular plasmon as a collective electronic excitation rather than a single-electron transition is supported by three primary attributes: (1) the strong dependence on the electron−electron interaction strength; (2) the excitation being a superposition of many elementary single-electron excitations (i.e., Slater determinants); and (3) the Coulomb potential from the plasmon-induced charges provides the dominant restoring force for the mode. These descriptions lead to the specific result predicted by Manjavacas et al.[17] that charged PAH molecules possess a set of molecular plasmon resonances that are remarkably sensitive to their charge state. As neutral molecules, PAHs exhibit large energy

Received: June 27, 2015
Revised: July 22, 2015
Published: August 5, 2015

DOI: 10.1021/acs.nanolett.5b02549
Nano Lett. 2015, 15, 6208−6214

gaps rendering most of them transparent in the visible range. Aromatic molecules possess overlapping π-orbitals, which provide them with remarkable chemical stability, resulting in six-membered benzene rings that support delocalized valence electrons. In an extended hexagonally packed lattice of such rings, the valence electrons recover the well-known band structure of graphene in which the electron mobility reaches high values when the material is doped with charge carriers, giving rise to metallic behavior supporting long-lived plasmons. Likewise, a discrete PAH molecule is predicted to support visible plasmons with the addition or removal of one or more electrons.[17] The added carrier in the PAHs plays only an indirect role in the plasmon motion. The addition of the extrinsic carrier changes the electronic structure of the molecule so that collective excitations become possible. The plasmon "motion" does not primarily involve the added carrier but is a coherent superposition of multiple electron−hole pair excitations involving the other electrons. This is in sharp contrast to plasmons in graphene, where the electrons forming the plasmon are the extrinsic dopants. In the limit of a very large system with a continuous electronic structure, the descriptions become equivalent.

The radical anions of PAH molecules are known to support visible resonances that in the past have been interpreted as single-electron excitations within the realm of molecular orbital theory.[23−25] The spectra we observe are consistent with those reported in the previous literature, confirming that the molecular plasmon is switched on by the addition of a single electron to the molecule and providing a radically new understanding of plasmon resonances in molecular-size systems. This finding represents an extrapolation of the high electrical tunability of nanographene plasmons to an extreme limit of spatial confinement, demonstrating a change of paradigm in plasmonics that holds great potential for visible light modulation.

This is illustrated in Figure 1a, which represents the electron density of the highest occupied molecular orbital (HOMO) of anthracene in its neutral and charged states, as well as the charge density induced upon resonant light irradiation, which constitutes the molecular plasmon.

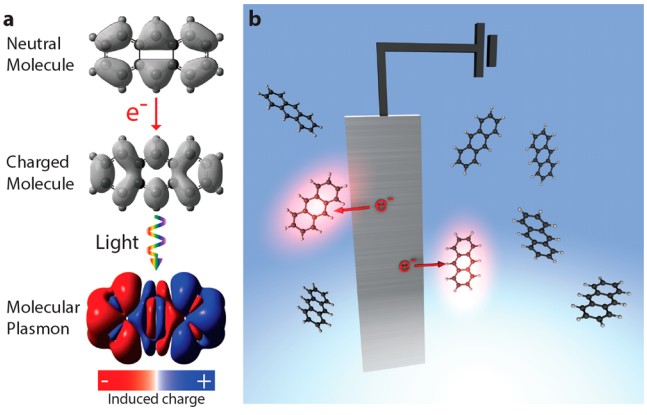

Figure 1. Molecular plasmons in electrically doped PAHs. (a) Upon addition of a single electron, the outer valence electron density of a neutral PAH molecule (upper panel) undergoes dramatic changes (central panel) that enable the excitation of a plasmon upon exposure to visible light (lower panel). We illustrate this concept with densities calculated from TDDFT for anthracene. (b) An electron is transferred from a metallic gate to dispersed molecules placed in its vicinity when the lowest unoccupied molecular orbital (LUMO) is tuned to the Fermi level of the gate. This process results in visible color changes of the solution.

To facilitate charge transfer to and from PAH molecules, a three-electrode electrochemical cell with optical access was designed (see Figure 1b and Supporting Information Figure S1), where current is passed through a nonaqueous electrolyte solution that contains a known concentration of PAH molecules. The PAH molecules were dissolved in dry organic solvent along with a supporting electrolyte and probed electrochemically. Electron transfer to the PAH molecules occurs at a Pt mesh working electrode, where the voltage is changed by passing an electrical current to and from an auxiliary electrode and measured relative to a Ag wire pseudoreference electrode. The addition and subsequent removal of an electron to the molecule is confirmed by the observation of reduction and reoxidation peaks in a cyclic voltammogram.[26,27] Optical measurements of the solution were obtained simultaneously with the electrochemical measurements, using white light illumination transmitted through the working electrode to a spectrometer, which continuously recorded the transmission spectrum. The color change during this process occurred across the full area of the 1 cm × 1 cm electrode, making the spectral changes easily observable to the naked eye. The present experimental setup does not allow the applications of sufficiently strong voltages to create the doubly negative charged anion or the positively charged cation. We are thus not able to verify the predicted scaling with charge (doping) density of the PAH molecules.

The absorbance spectra of isomeric three- and four-unit planar aromatic ring molecules in tetrahydrofuran (THF) were measured in their neutral and negatively charged states (Figure 2). In their neutral state, these molecules have well-known electronic absorption bands in the near-UV, corresponding to HOMO−LUMO transitions.[28] In particular, the linear four-ring molecules, tetracene and tetraphene, have comparatively lower energy gaps, resulting in a noticeable yellow tint of the neutral solution. At the first reduction potential, the molecules accept a single electron. This creates a negatively charged radical anion and a dramatic color change (Figure 2a), corresponding to the excitation of a resonance that dominates the visible absorption spectra (Figure 2b). The energy of the peak resonance in the experimental data is in excellent agreement with results from TDDFT calculations, as can be seen by comparing the peak positions in Figure 2b,c (see Methods and Supporting Information for more details).

In contrast to larger graphene nanostructures, the PAH absorption spectra possess a rich and complex fine structure. A series of side bands are observable at higher energies with respect to each primary absorption peak virtually in all molecules studied. We attribute these additional bands to the coupling between the molecular plasmon (i.e., the primary peak) and the vibrational modes of the molecules. This hypothesis is well supported by theoretical calculations of the vibrationally resolved absorption spectrum (Figure 3), which are in excellent qualitative agreement with the structure of the experimentally measured spectra for both anthracene and tetracene (see Methods for details of the calculation method). Clearly the agreement between theory and experiment is not as good as we typically obtain for conventional metallic nanoparticle plasmonic structures. There are a number of possible reasons: first, the theoretical formalism underlying vibrational couplings are much more complex and incomplete than for

DOI: 10.1021/acs.nanolett.5b02549
Nano Lett. 2015, 15, 6208−6214

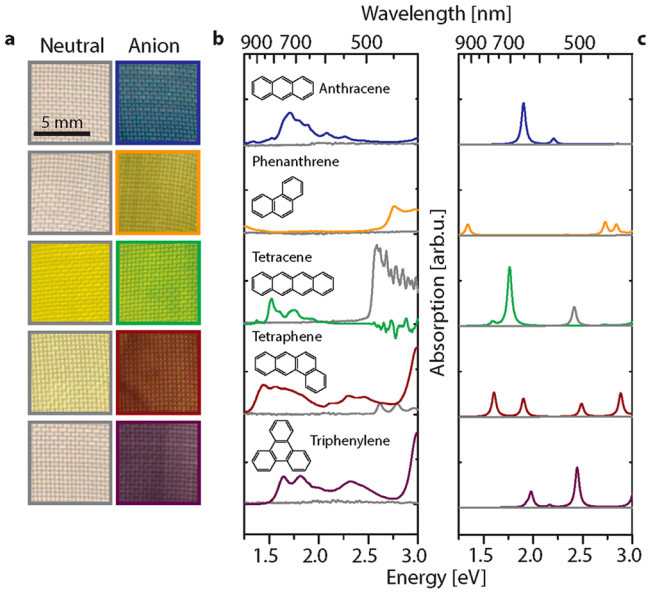

Figure 2. Electrical tunability of visible light absorption in PAHs. Five different PAHs are studied (from top to bottom): anthracene, phenanthrene, tetracene, tetraphene, and triphenylene. All solutions contain 5 mM PAH in THF with 500 mM supporting electrolyte. (a) Visible images of the PAH solution in the neutral state (left, gray borders) and −1 charge state (right, colored borders) for each molecule. (b) Measured absorption spectra for the neutral (gray) and −1 charge-state (colored) PAH molecules. (c) TDDFT calculated spectra for the PAH molecules in THF.

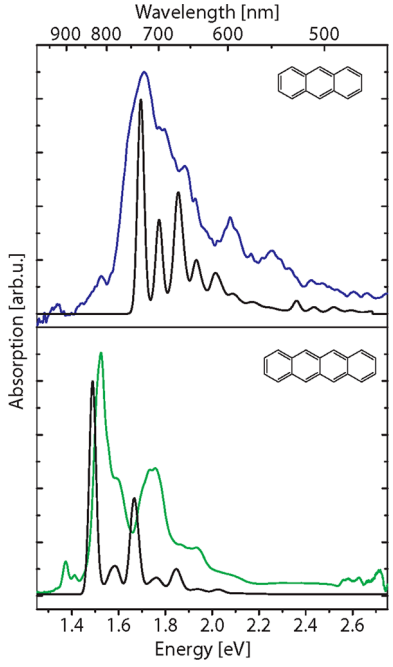

Figure 3. Vibrationally resolved absorption spectra. We show a comparison between measured spectra (colored curves) and theoretical calculations (black curves) including coupling to vibrational sublevels for two representative singly charged PAHs (anthracene and tetracene), both in THF.

classical electromagnetic simulations; second, the experiment involves ensembles of PAH molecules that may both couple to the solvent molecules and to each other; third, the vibrationally resolved theoretical spectra take into account only the strongest transition peak for each molecule within the spectral region considered. However, as seen in Figure 2, both anthracene and tetracene possess additional weaker peaks within ∼0.5 eV of the strongest peak. These modes can also couple to molecular vibrational modes and give rise to further (but less pronounced) structure in the vibration sidebands.

The strength of the plasmon coupling to light is an important parameter that determines the concentration of molecules required for practical applications (e.g., visible light modulation and switching). As the measured plasmon is likely broadened by interaction with the stochastic distribution of solvent molecules (e.g., through averaging over local frequency shifts or via coupling to inelastic modes of the liquid), we assess the noted coupling by examining the spectral integral of the absorption cross-section over each plasmon + satellites region. This magnitude should be roughly independent of the type of solvent and the presence of different inelastic loss channels. In practice, we measure the absorption cross-section for the anthracene molecular plasmon by recording the maximum absorbance (at ∼1.71 eV) as a function of time upon application of a constant potential, a method known as chronoabsorptometry (see Methods); the molar absorptivity obtained using this approach is nominally 3 500 M^{-1} cm^{-1}, translating into an absorption cross-section of 6 × 10^{-4} nm^2. The molar absorptivity we obtain is similar to but slightly lower than that of the neutral molecular absorption of anthracene, which is 6 200 M^{-1} cm^{-1} at ∼3.44 eV. From this calibration of the absorption maximum, we now integrate the spectrum and obtain a peak area of 2.3 × 10^{-4} nm^2 eV, which compares reasonably well with the theoretical prediction of 14.8 × 10^{-4} nm^2 eV.

Because the resonant frequencies of metallic surface plasmons are highly sensitive to size, shape, and surrounding dielectric environment, we examine these same dependences in molecular plasmons (Figure 4). The molecular plasmon resonances redshift with increasing molecule length from ∼930 pm (anthracene, absorption peak at 1.71 eV, Figure 4a) to ∼1180 pm (tetracene, absorption peak at 1.52 eV, Figure 4c). This correlation is analogous to the nearly linear relationship between metal nanorod plasmon wavelength and nanorod length and is in agreement with the effect of spatial confinement of a charge distribution.[22,29] We also observed a linear redshift with increasing index of refraction of the surrounding environment.[30] Spectra of the negatively charged PAHs were recorded for solutions in a series of organic solvents with increasing indices of refraction (Figure 4b,d). The anthracene anion was measured in six separate solvents: MeCN (acetonitrile, n = 1.3441), THF (n = 1.4072), PC (propylene carbonate, n = 1.4189), DMF (dimethylformamide, n = 1.4305), DMSO (dimethyl sulfoxide, n = 1.4793), and pyridine (n = 1.509). The tetracene anion was measured in three solvents (THF, DMF, and pyridine). The nine normalized spectra corresponding to this solvent shift are shown in Figure 4a,c. We also observe that the spectra of both anthracene and tetracene molecular plasmons are modified to a greater degree in pyridine than in the other solvents: for anthracene, a substantially broadened spectrum is observed, while for tetracene an additional broad spectral shoulder from 2.0 to 2.6 eV appears. This may indicate an enhanced interaction or affinity between the molecular plasmon and the pyridine solvent molecules, which are also aromatic rings (C_5H_5N), and possess substantial vibrational mode overlap with the plasmonic molecules.

DOI: 10.1021/acs.nanolett.5b02549
Nano Lett. 2015, 15, 6208−6214

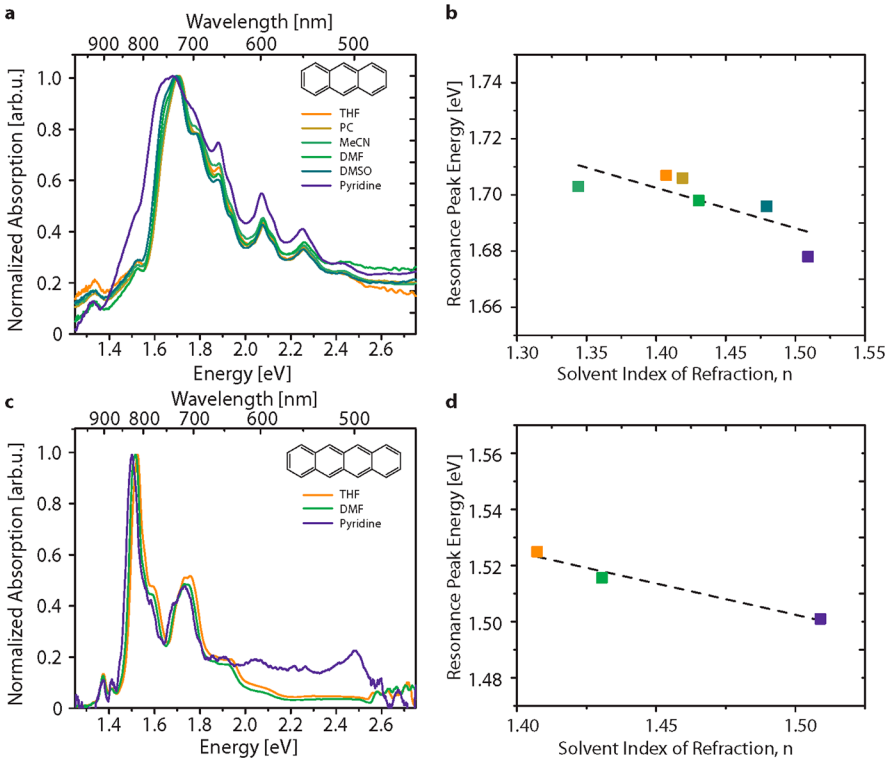

Figure 4. Tunability of the molecular plasmon. (a,c) The peak energy of the plasmon resonance can be red-shifted by increasing the dielectric constant of the environment. (b,d) The peak energy of the leading spectral maximum in (a,c) is shown to redshift linearly with increasing index of refraction. This figure also illustrates the resonance redshift when increasing the length of the molecule from ∼930 pm for anthracene (a) to ∼1180 pm for tetracene (c).

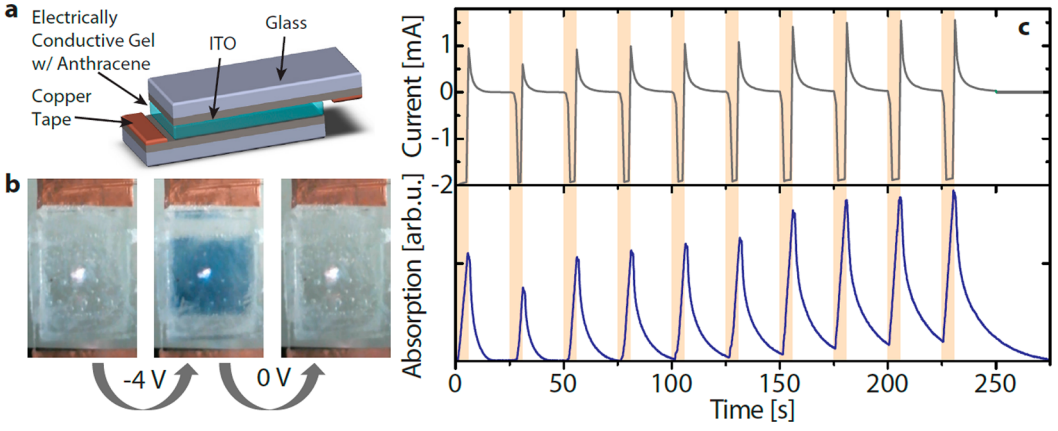

Figure 5. A molecular plasmon electrochromic device. A symmetric ITO−anthracene gel−ITO device was constructed (a) which exhibits a reversible color change upon application and removal of voltage (b). The active area of the device is ∼1 cm × 1 cm. The white spot in the middle is the specular reflection of the illumination source for the spectroscopic measurements. (c) The color change continues through multiple voltage switching cycles between −4 V (for 5s, illustrated by the orange bands in panel c) and 0 V (for 20s). The absorbance is measured at 1.71 eV (the molecular plasmon peak resonance for anthracene) and can be seen to turn off completely after sufficient time upon removal of voltage.

As a proof-of-principle for molecular plasmonic applications, we have prepared a symmetric electrochromic device by dissolving anthracene in an electrically conductive transparent polymer gel and laminating it between two pieces of a transparent conductive oxide as shown in the schematic of Figure 5a. The long-lived visible color (many seconds) and repeatable switching (more than 10 cycles in our initial test) demonstrate the viability of this concept (see Figure 5b,c). The extinction spectrum of the device is extremely similar to the extinction of the singly charged anthracene anion in solution obtained in the electrochemical cell, as shown in Supporting Information Figure S6. Water and impurities in the solution result in some discoloration from byproduct formation with successive switching cycles. However, we have verified that reasonable attempts to reduce water content and impurities can significantly improve this performance. Optimization of the conductive polymer[31] and electrodes[32] should result in further improvements in transmission, cycling endurance, and switching speed.

The excitations here studied involve collective motion of several electrons driven by their mutual Coulomb interaction, and thus we brand them as molecular plasmons, governed by

DOI: 10.1021/acs.nanolett.5b02549
Nano Lett. 2015, 15, 6208−6214

the same principles as their plasmonic excitation counterparts sustained by larger PAHs (eventually reaching nanographene sizes) and metallic nanoparticles. This insight paves the way for using PAHs in new applications relying on plasmonic rather than excitonic properties. For instance, because these excitations involve strong induced charge densities, the field enhancements can be made larger, which may have implications for sensing applications. Additionally, as the plasmon is sustained by long-range Coulomb interactions, it may be possible to use PAH molecules in waveguiding and energy transfer applications.

Our experimental observations confirm the existence of molecular plasmons in charged aromatic molecules[17] and establish this system as a stable medium that is switchable between transparency and vivid absorption at safe, easily accessible voltages in electrolytic environments. Because this dramatic change in optical absorption is triggered by a single electron transfer process, we anticipate that it is likely to be a fundamentally fast process at the molecular scale, analogous to the subpicosecond charge transfer processes proposed for plastic solar cells.[33] Unlike other better-known but far slower electrochromic mechanisms, devices based on switchable molecular plasmons could ultimately find use as optical filters and shutters in a range of consumer applications. The natural abundance, low cost, and extremely large variety of PAH molecules available could make extremely large-area active color-switching applications, such as walls, windows, or other architectural elements, and even vehicles, a practical technology.

Methods. *Solution Preparation.* All PAH molecules, anthracene, tetracene, tetraphene, phenanthrene, triphenylene, and supporting electrolyte tetrabutylammonium perchlorate (TBAP), were purchased from Sigma-Aldrich and purified via recrystallization from diethyl ether. Dimethylformamide, propylene carbonate, and dimethyl sulfoxide were purchased from Sigma-Aldrich and purified using vacuum distillation and/or the freeze−pump−thaw method. Tetrahydrofuran, pyridine, and acetonitrile were purchased from Sigma-Aldrich and purified through a high-pressure solvent purification system. Karl Fischer titration of all solvents showed less than 50 ppm water impurity. Solutions for electrochemical measurements contained 5 mM of the PAH under investigation with 500 mM of supporting electrolyte (tetrabutyl ammonium perchlorate, TBAP), unless otherwise noted. All solutions were prepared, stored, and transferred under inert (N_2 or Ar gas) conditions.

Spectroelectrochemical Measurements. A three-electrode measurement is taken using platinum mesh working- and counter-electrodes with a Ag-wire pseudoreference electrode. Ag wire is used due to the nonaqueous conditions to prevent side reactions from occurring between PAH anions and ions leaked from a conventional reference electrode. In order to compare measured reduction potentials against reported values, the Ag wire pseudoreference electrode is externally calibrated against the ferrocene redox couple[34] (Fc/Fc+). All reduction potentials are reported relative to this value. The reduction and reoxidation occur at approximately −2.20 V and −1.15 V versus Fc/Fc+ (see Supporting Information Figure S2), respectively, for anthracene in THF. The measured reduction potential for the tested molecules is consistently in agreement with previously reported experimental values.[35,36] The electrochemical potential ranges accessible in many organic solvents readily support the reduction of small PAHs and the observation of their (−1) molecular plasmon. Absorption measurements are taken concurrently with voltage sweeps using a white light source (dual lamps: halogen and laser-driven plasma) incident on the working electrode, transmitted to the spectrometer where the spectrum is recorded.

Chronoabsorptometry. This measurement is nearly identical to the spectroelectrochemical measurements except that an ITO-covered glass slide (Delta Technologies, 15−25 Ω) was used as the working electrode. The change in optical absorption is directly proportional to the change in measured current, both of which are linear for short time scales (within the first few seconds after applying the potential). The molar absorptivity of the reduced state can be derived by substituting the Cottrell equation (for current in an electrochemical cell as a function of time and neutral analyte concentration) into Beer's law.[37] We used the diffusion coefficient calculated from the measured current over the same time period as the absorption was measured so that, as expected, the diffusion constant remained uniform over the calculation region. The molar absorptivity of neutral and charged anthracene was obtained for solutions in DMF with 100 mM TBAP as the supporting electrolyte.

Device Preparation and Measurement. Anthracene, supporting electrolyte tetrabutylammonium hexafluorphosphate (TBAPF6), and poly(methyl methacrylate) (PMMA), average $M_w \sim 996\,000$, were purchased from Sigma-Aldrich and purified by means of recrystallization from THF. The conductive gel was prepared by dissolving 80 mM anthracene, 80 mM TBAPF6, and 10 wt % PMMA in THF under dry argon flow and stirring overnight. The gel was dropcast onto two ITO-covered glass slides (Sigma-Aldrich, 8−12 Ω/sq) in a dry N_2 glovebox and allowed to cure for 8 min before sandwiching the two ITO/glass slides together. A 360 μm thick adhesive (Grace Biolabs SecureSeal) was used as a spacer layer and an adhesive layer for the two slides. Cu-tape and Ag wire were used to connect the ITO surfaces to the potentiostat for a two-electrode measurement. All other electrical and optical measurements for this device were performed in the same manner as described in the Spectroelectrochemical Measurement and Chronoabsorptometry paragraphs.

Theoretical Calculations. All theoretical calculations were performed using *Gaussian 09*.[38] We performed DFT calculations to optimize the molecular geometry and computed the ground state properties (e.g., electron affinity and vibrational modes). We used the hybrid B3LYP functional and the 6-31+G(d) basis set consisting of a valence double-ζ basis set complemented with s and p diffuse functions, as well as d polarization functions for the carbon atoms. The choice of the functional and the basis set is consistent with previous works[39,40] in which the suitability of different basis sets to describe the response of PAHs was analyzed. The absorption spectra and the induced charge density distributions were obtained using TDDFT with the same combination of functional and basis set. The effect of the solvent was incorporated in all calculations using the polarizable continuum model.[38] The vibrationally resolved absorption spectra were calculated following the procedure developed by Barone et al.,[41] which relies on the Franck−Condon principle to obtain the strength of the transitions between the vibrational levels of the ground and the excited electronic states.

DOI: 10.1021/acs.nanolett.5b02549
Nano Lett. 2015, 15, 6208−6214

■ ASSOCIATED CONTENT

Supporting Information

The Supporting Information is available free of charge on the ACS Publications website at DOI: 10.1021/acs.nanolett.5b02549.

The spectroelectrochemical experimental setup for the electrochemical measurements, cyclic voltammogram with and without anthracene, spectroelectrochemical measurements as a function of electrolyte concentration, anthracene plasmon switching endurance (multiple cycling) in electrochemical cell, and spectrum of anthracene plasmon electrochromic device. (PDF)

■ AUTHOR INFORMATION

Corresponding Authors

*E-mail: (G.d.A.): javier.garciadeabajo@icfo.es.
*E-Mail: (P.N.): nordland@rice.edu.
*E-Mail: (N.J.H.): halas@rice.edu.

Author Contributions

A.L., A.E.S, A.M., and Y.C. contributed equally to this work. A.L. and A.E.S. performed most experiments and performed data analysis. A.L. and M.M. produced most of the solutions. A.L. and G.S. constructed and tested the electrochromic gel device. Y.C. and A.M. performed the theoretical modeling and calculations. F.J.G.A., P.N., and N.J.H. conceived the project and supervised the research. All authors contributed to the development of the manuscript.

Notes

The authors declare no competing financial interest.

■ ACKNOWLEDGMENTS

We thank Alejandro J. Garza for helpful and enjoyable discussions. A.M. acknowledges financial support from the Welch foundation through the J. Evans Attwell-Welch Postdoctoral Fellowship Program of the Smalley-Curl Institute of Rice University (Grant L-C-004). This work was also supported by the Robert A. Welch Foundation under Grant C-1220 (N.J.H.) and C-1222 (P.N.) and by the Office of Naval Research under Grant N00014-10-0989. F.J.G.A. acknowledges support from the Spanish MINECO (MAT2014-59096-P).

■ REFERENCES

(1) Maier, S. A. *Plasmonics: Fundamentals and Applications: Fundamentals and Applications*; Springer: New York, 2007; http://books.google.com/books?id=yT2ux7TmDc8C&pgis=1.
(2) Camden, J. P.; Dieringer, J. A.; Zhao, J.; Van Duyne, R. P. Controlled plasmonic nanostructures for surface-enhanced spectroscopy and sensing. *Acc. Chem. Res.* **2008**, *41*, 1653−61.
(3) Knight, M. W.; Sobhani, H.; Nordlander, P.; Halas, N. J. Photodetection with active optical antennas. *Science* **2011**, *332*, 702−4.
(4) Fei, Z.; et al. Infrared nanoscopy of dirac plasmons at the graphene-SiO2 interface. *Nano Lett.* **2011**, *11*, 4701−4705.
(5) Ju, L.; et al. Graphene plasmonics for tunable terahertz metamaterials. *Nat. Nanotechnol.* **2011**, *6*, 630−634.
(6) Chen, J.; et al. Optical nano-imaging of gate-tunable graphene plasmons. *Nature* **2012**, *487*, 77−81.
(7) Fang, Z.; et al. Active tunable absorption enhancement with graphene nanodisk arrays. *Nano Lett.* **2014**, *14*, 299−304.
(8) Koppens, F. H. L.; Chang, D. E.; García de Abajo, F. J. Graphene plasmonics: a platform for strong light-matter interactions. *Nano Lett.* **2011**, *11*, 3370−7.
(9) Grigorenko, A. N.; Polini, M.; Novoselov, K. S. Graphene plasmonics. *Nat. Photonics* **2012**, *6*, 749−758.
(10) Yan, H.; et al. Damping pathways of mid-infrared plasmons in graphene nanostructures. *Nat. Photonics* **2013**, *7*, 394−399.
(11) Fang, Z.; et al. Gated tunability and hybridization of localized plasmons in nanostructured graphene. *ACS Nano* **2013**, *7*, 2388−95.
(12) Fei, Z.; et al. Gate-tuning of graphene plasmons revealed by infrared nano-imaging. *Nature* **2012**, *487*, 82−5.
(13) Liu, L.; Han, Z.; He, S. Novel surface plasmon waveguide for high integration. *Opt. Express* **2005**, *13*, 6645.
(14) Lee, J.; Mubeen, S.; Ji, X.; Stucky, G. D.; Moskovits, M. Plasmonic photoanodes for solar water splitting with visible light. *Nano Lett.* **2012**, *12*, 5014−9.
(15) Manjavacas, A.; Thongrattanasiri, S.; García de Abajo, F. J. Plasmons driven by single electrons in graphene nanoislands. *Nanophotonics* **2013**, *2*, 139−151.
(16) García de Abajo, F. J. Graphene Plasmonics: Challenges and Opportunities. *ACS Photonics* **2014**, *1*, 135−152.
(17) Manjavacas, A.; et al. Tunable Molecular Plasmons in Polycyclic Aromatic Hydrocarbons. *ACS Nano* **2013**, *7*, 3635−43.
(18) Guidez, E. B.; Aikens, C. M. Origin and TDDFT Benchmarking of the Plasmon Resonance in Acenes. *J. Phys. Chem. C* **2013**, *117*, 21466−21475.
(19) Bursi, L.; Calzolari, A.; Corni, S.; Molinari, E. Light-induced field enhancement in nanoscale systems from first-principles: the case of polyacenes. *ACS Photonics* **2014**, *1*, 1049.
(20) Bernadotte, S.; Evers, F.; Jacob, C. R. Plasmons in Molecules. *J. Phys. Chem. C* **2013**, *117*, 1863−1878.
(21) Thongrattanasiri, S.; Manjavacas, A.; García de Abajo, F. J. Quantum finite-size effects in graphene plasmons. *ACS Nano* **2012**, *6*, 1766−75.
(22) Krauter, C. M.; Schirmer, J.; Jacob, C. R.; Pernpointner, M.; Dreuw, A. Plasmons in molecules: Microscopic characterization based on orbital transitions and momentum conservation. *J. Chem. Phys.* **2014**, *141*, 104101.
(23) Shida, T.; Iwata, S. Electronic spectra of ion radicals and their molecular orbital interpretation. III. Aromatic hydrocarbons. *J. Am. Chem. Soc.* **1973**, *95*, 3473−3483.
(24) Hoijtink, G. J. Correlations between the electronic spectra of alternant hydrocarbon molecules and their mono- and di-valent ions II. *Mol. Phys.* **1960**, *2*, 85−95.
(25) Balk, P.; Hoijtink, G. J.; Schreurs, J. W. H. Electronic spectra of mono- and di-negative aromatic ions. *Recl. des Trav. Chim. des Pays-Bas* **1957**, *76*, 813−823.
(26) Heinze, J. Cyclic Voltammetry—'Electrochemical Spectroscopy'. New Analytical Methods(25). *Angew. Chem., Int. Ed. Engl.* **1984**, *23*, 831−847.
(27) Santhanam, K. S. V.; Bard, A. J.; Unioersity, T. The Electrochemical Reduction of 9,10-Diphenylanthracene. *J. Am. Chem. Soc.* **1966**, *88*, 2669−2675.
(28) Hoijtink, G. J.; Zandstra, P. J. Polarization of electronic transitions in aromatic hydorcarbon molecules and their mono- and di-valent ions. *Mol. Phys.* **1960**, *3*, 371−389.
(29) Novotny, L. Effective Wavelength Scaling for Optical Antennas. *Phys. Rev. Lett.* **2007**, *98*, 266802.
(30) Kelly, K. L.; Coronado, E.; Zhao, L. L.; Schatz, G. C. The Optical Properties of Metal Nanoparticles: The Influence of Size, Shape, and Dielectric Environment. *J. Phys. Chem. B* **2003**, *107*, 668−677.
(31) Thakur, V. K.; Ding, G.; Ma, J.; Lee, P. S.; Lu, X. Hybrid materials and polymer electrolytes for electrochromic device applications. *Adv. Mater.* **2012**, *24*, 4071−96.
(32) Sun, X. W.; Wang, J. X. Fast switching electrochromic display using a viologen-modified ZnO nanowire array electrode. *Nano Lett.* **2008**, *8*, 1884−9.
(33) Kraabel, B.; McBranch, D.; Sariciftci, N.; Moses, D.; Heeger, A. Ultrafast spectroscopic studies of photoinduced electron transfer from semiconducting polymers to C60. *Phys. Rev. B: Condens. Matter Mater. Phys.* **1994**, *50*, 18543−18552.
(34) Bond, A. M.; Oldham, K. B.; Snook, G. A. Use of the Ferrocene Oxidation Process To Provide Both Reference Electrode Potential

DOI: 10.1021/acs.nanolett.5b02549
Nano Lett. 2015, 15, 6208−6214

Calibration and a Simple Measurement (via Semiintegration) of the Uncompensated Resistance in Cyclic Voltammetric Studies in High-Resistance Organic Solvents. *Anal. Chem.* **2000**, *72*, 3492−3496.
(35) Kubota, T.; Kano, K.; Uno, B.; Konse, T. Energetics of the sequential electroreduction and electrooxidation steps of benzenoid hydrocarbons. *Bull. Chem. Soc. Jpn.* **1987**, *60*, 3865−3877.
(36) Amatore, C.; Lefrou, C.; Pflüger, F. On-line compensation of ohmic drop in submicrosecond time resolved cyclic voltammetry at ultramicroelectrodes. *J. Electroanal. Chem. Interfacial Electrochem.* **1989**, *270*, 43−59.
(37) Kissinger, P. T.; Heineman, W. R. *Laboratory techniques in electroanalytical chemistry*; Kissinger, P. T., Heineman, W. R., Eds.; Marcel Dekker: New York, 1996.
(38) Frisch, M. J.; et al. *Gaussian 09*, revision A.02.; Gaussian, Inc.: Wallingford, CT, 2009.
(39) Malloci, G.; Mulas, G.; Cappellini, G.; Joblin, C. Time-dependent density functional study of the electronic spectra of oligoacenes in the charge states − 1, 0, + 1, and + 2. *Chem. Phys.* **2007**, *340*, 43−58.
(40) Malloci, G.; Cappellini, G.; Mulas, G.; Mattoni, A. Electronic and optical properties of families of polycyclic aromatic hydrocarbons: A systematic (time-dependent) density functional theory study. *Chem. Phys.* **2011**, *384*, 19−27.
(41) Barone, V.; Bloino, J.; Biczysko, M.; Santoro, F. Fully Integrated Approach to Compute Vibrationally Resolved Optical Spectra: From Small Molecules to Macrosystems. *J. Chem. Theory Comput.* **2009**, *5*, 540−554.

DOI: 10.1021/acs.nanolett.5b02549
Nano Lett. 2015, 15, 6208−6214

MOLECULAR PLASMONICS

Supplemental Information

Adam Lauchner,[1,6]* *Andrea E. Schlather*,[2,6]* *Alejandro Manjavacas*,[3,6*] *Yao Cui*,[2,6*] *Michael J. McClain*,[2,6] *Grant Stec*,[2,6] *F. Javier García de Abajo*,[4,5] *Peter Nordlander*,[1,3,6] *and Naomi J. Halas*[1,2,3,6]

[1]Department of Electrical and Computer Engineering, Rice University, Houston, TX, USA
[2]Department of Chemistry, Rice University, Houston, TX, USA
[3]Department of Physics and Astronomy, Rice University, Houston, TX, USA
[4]ICFO-Institut de Ciencies Fotoniques, Mediterranean Technology Park, 08860 Castelldefels (Barcelona), Spain
[5]ICREA-InstitucióCatalana de Recerca i Estudis Avancats, Passeig Lluís Companys, 23, 08010 Barcelona, Spain
[6]Laboratory for Nanophotonics, Rice University Houston, TX, USA

*** Author contributions:**
These Authors contributed equally to this work.
Correspondence and requests for materials should be addressed to N.J.H. (email: halas@rice.edu).

Electrochemical Measurements

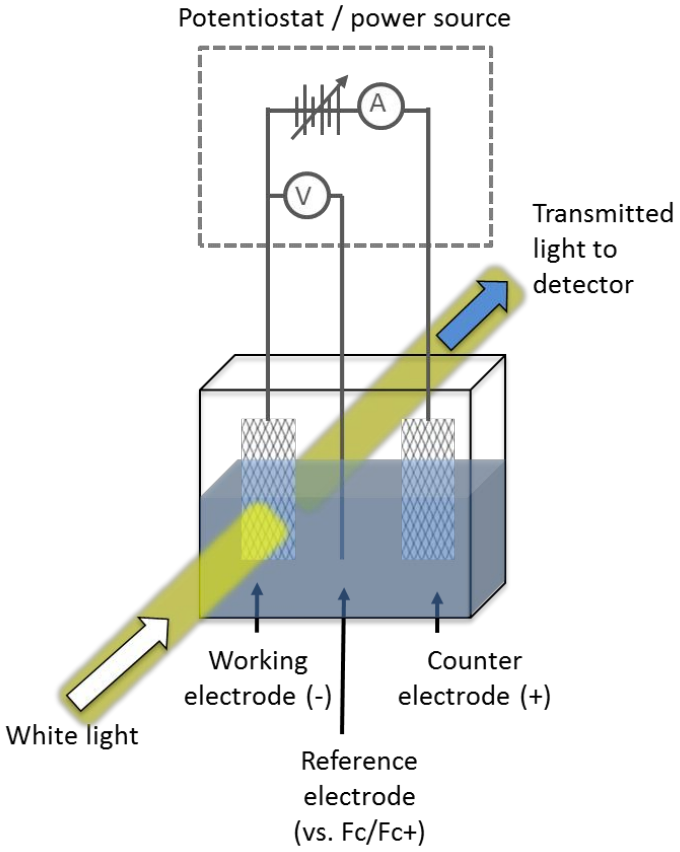

Figure S1: Spectroelectrochemical Setup. A three-electrode electrochemical cell configuration forms a complete circuit, controlled by potentiostat. White light is transmitted through the working electrode and recorded by a spectrometer. For the measurements conducted in this manuscript, the working electrode was always set as the negative voltage. The solution in the cell consists of 500 mM supporting electrolyte and 5mM PAH molecule in a dry organic solvent purged with argon.

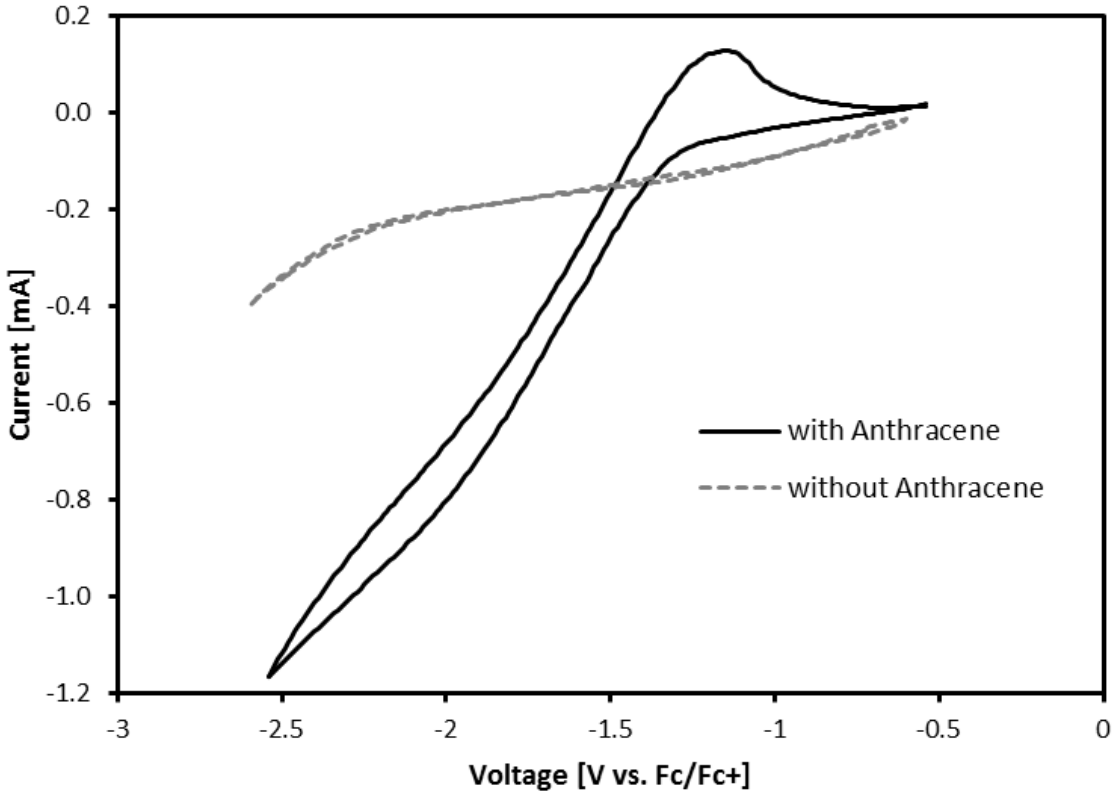

Figure S2: Cyclic Voltammogram. Current measured as a function of voltage sweep for THF (with 500 mM TBAP) both with 5mM Anthracene (solid, black line) and without Anthracene (dashed, grey line).

Spectroscopic Measurements and Simulations

The shape of the absorption band in tetracene above ~ 2.75 eV in Figure 2b is unreliable due to the concentration of the neutral solution. The HOMO-LUMO transition is strongly absorbing, resulting in low transmission at that energy for a 5mM solution with a 10mm topical path length and a weak, noisy signal for the anion when the neutral spectrum was subtracted from the total measured spectrum. Also, the apparent discrepancy between the heights of the neutral and anion peaks for tetracene compared to theory is due to the differences in concentration between the anion and the neutral molecule (concentration of anion was much lower than the concentration of the neutral molecule). The diffusion length around the electrode is much less than the 10mm optical path length; thus, even when the electrode was saturated with charged molecules, only a small fraction of the total molecules along the optical path were charged.

On the theory side, it has been shown that TDDFT calculations of the absorption spectrum of PAHs are limited to an accuracy of few tens of meV on the resonance peak positions when compared to experimental data.[1–3] Further, the spectra shown in Figure 2c do not include the fine detail due to vibrational coupling, which is expanded in greater detail in Figure 3, and which results in an excellent agreement between theory and experiment.

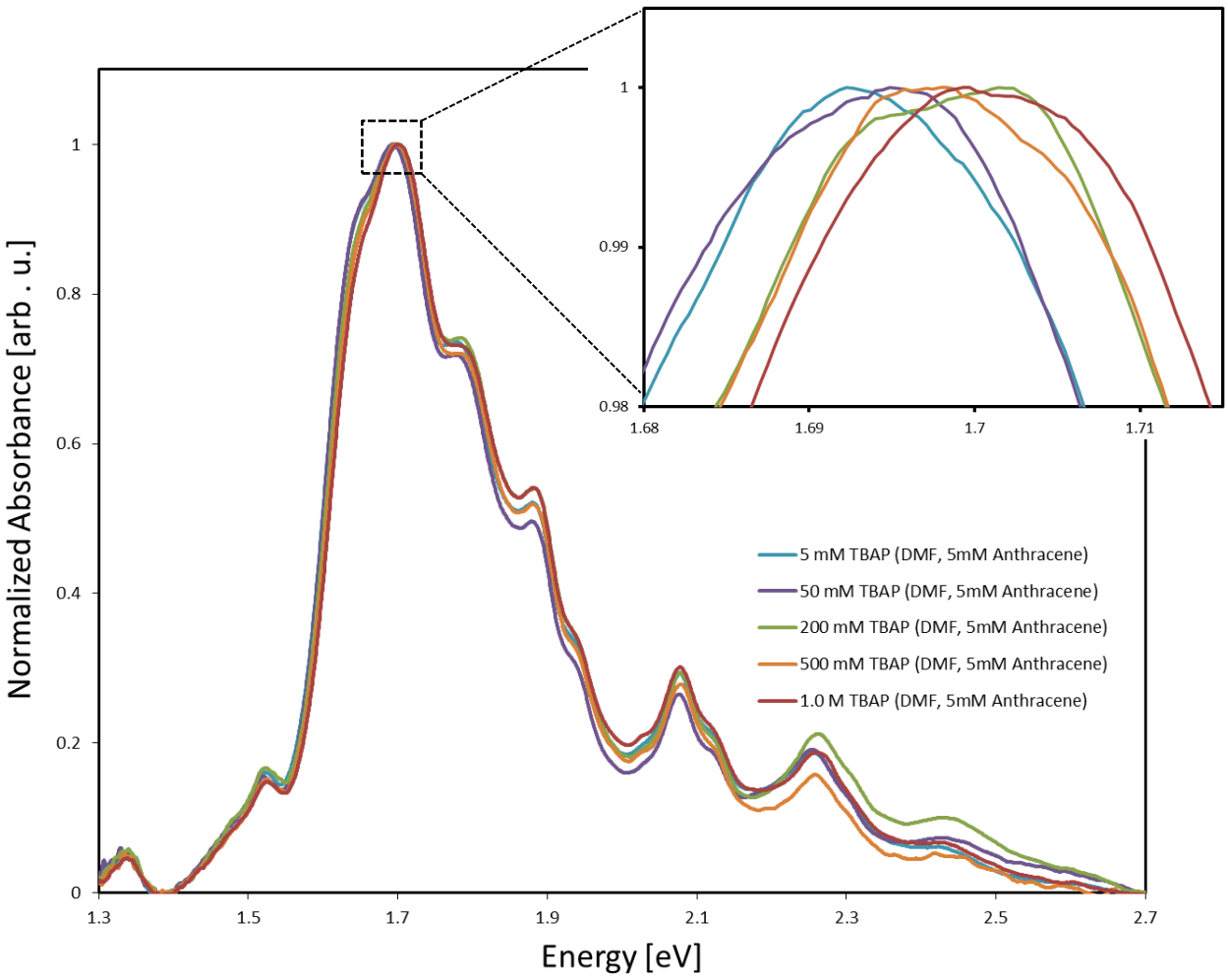

Figure S3: Electrolyte Concentration. The electrolyte concentration was varied from 5mM to 1,000 mM at constant Anthracene concentration (in DMF). While the system response is slightly slower at lower electrolyte concentration, the energy of the peak resonance redshifts only very slightly with increasing concentration.

Electrochemical Endurance

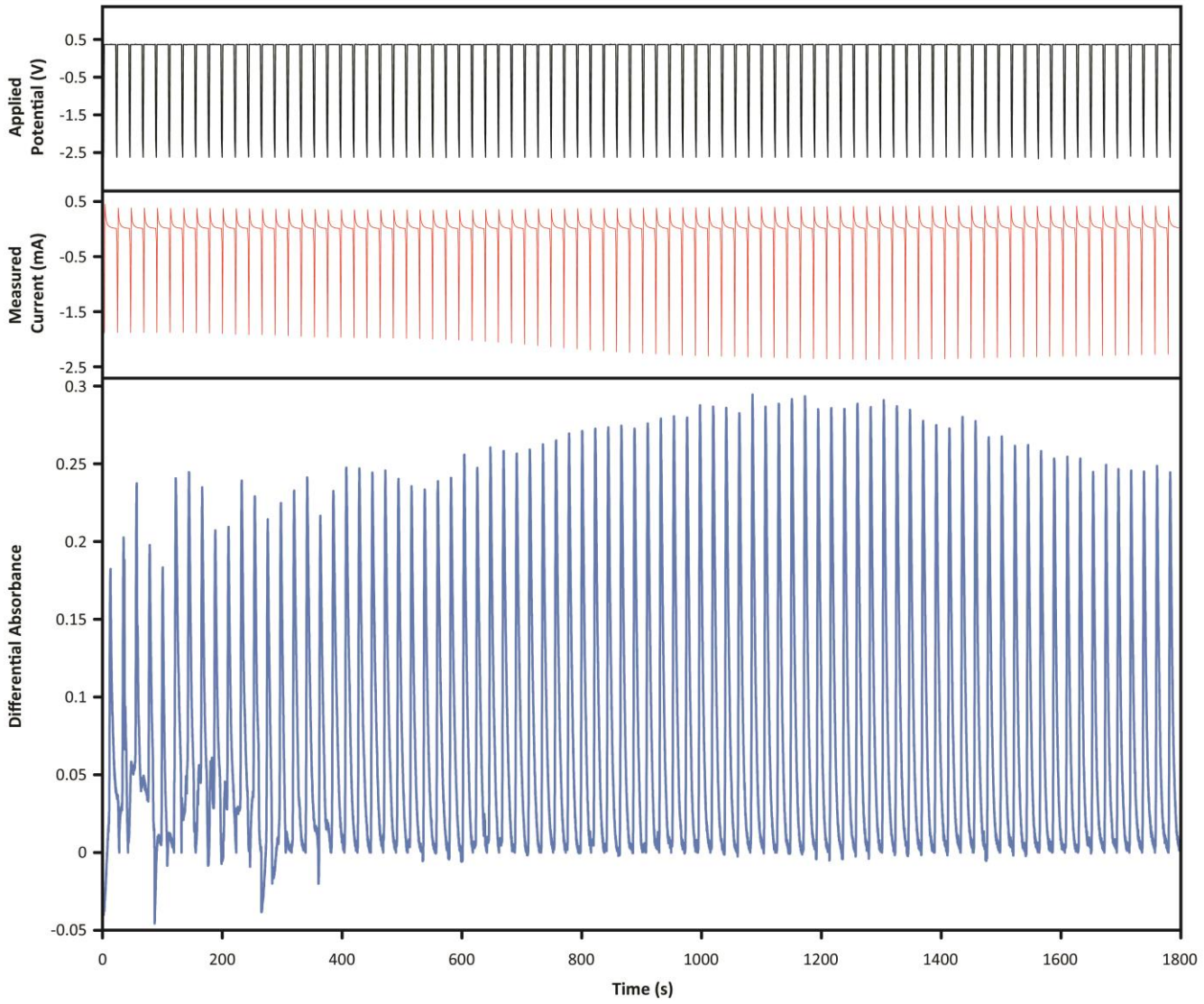

Figure S4: Plasmon switching endurance in electrochemical cell. A 10 mM Anthracene solution (in THF, 500 mM TBAP) was monitored spectroscopically during alternating applied voltages of -2.6 V for 3s and 0.4 V (vs. Fc/Fc+) for 20 seconds, over the course of 30 minutes. The differential absorbance during this period is plotted as measured at 1.71 eV (i.e., at the peak resonance of the molecule plasmon in Anthracene).

Electrochromic Device Spectrum

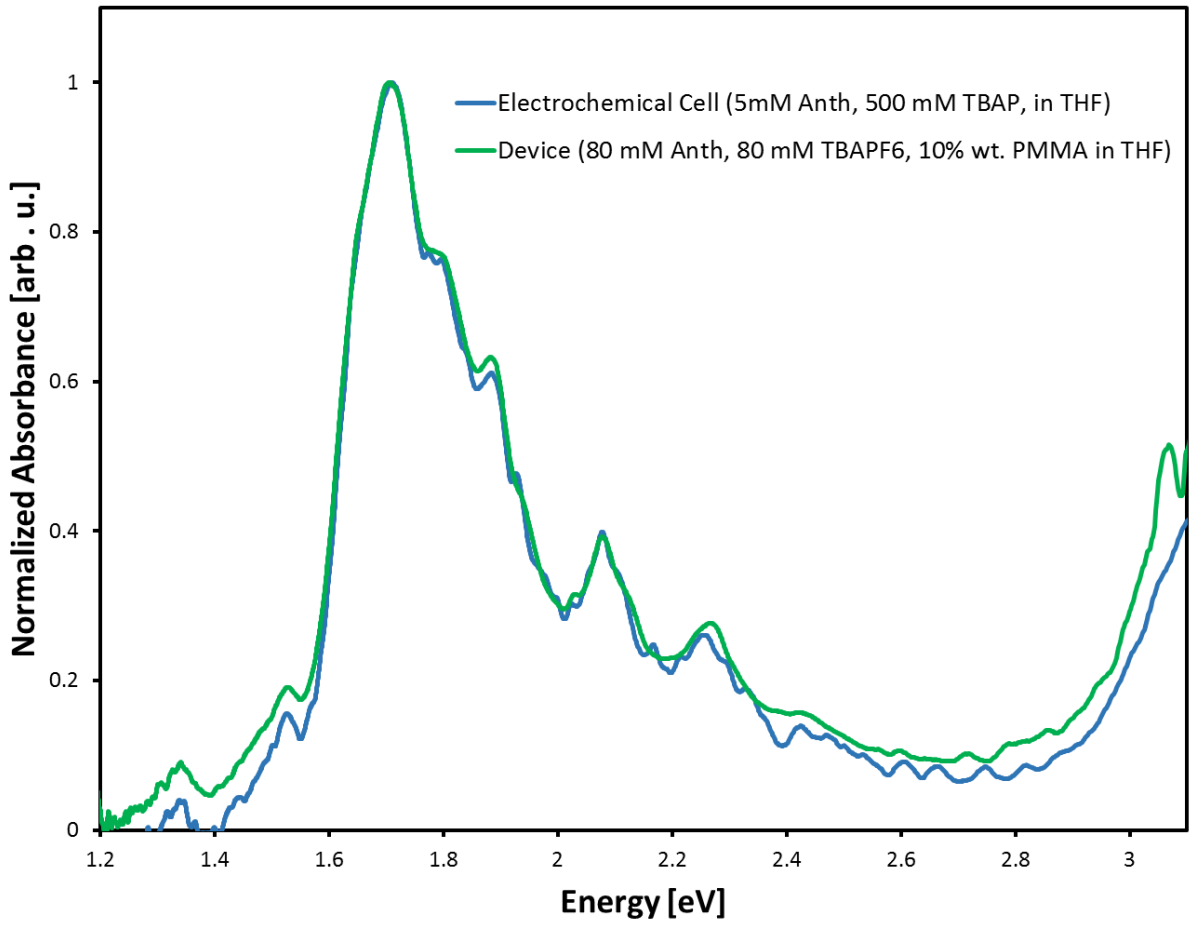

Figure S5: Comparison of solution-state and gel device molecular plasmon spectra. Normalized absorption spectra of the anthracene anion molecular plasmon as recorded in solution with the electrochemical cell (blue curve) and the ITO-anthracene gel-ITO device.

References

1. Dominikowska, J., Domagala, M. & Palusiak, M. UV-vis spectra of singlet state cationic polycyclic aromatic hydrocarbons : Time- dependent density functional theory study UV-vis spectra of singlet state cationic polycyclic aromatic hydrocarbons : Time-dependent density functional theory study. **044324,** (2014).

2. Malloci, G., Cappellini, G., Mulas, G. & Mattoni, A. Electronic and optical properties of families of polycyclic aromatic hydrocarbons: A systematic (time-dependent) density functional theory study. *Chem*. *Phys*. **384,** 19–27 (2011).

3. Malloci, G., Mulas, G., Cappellini, G. & Joblin, C. Time-dependent density functional study of the electronic spectra of oligoacenes in the charge states −1, 0, +1, and +2. *Chem*. *Phys*. **340,** 43–58 (2007).